J Eng Math (2008) 62:223–232
DOI 10.1007/s10665-008-9215-5

Thermal-stress analysis of plates with variable fiber spacing

Chung-Li Hwan

Received: 17 October 2006 / Accepted: 28 January 2008 / Published online: 14 February 2008

Abstract Plane-stress problems of a square composite plate with variable fiber spacing under a uniform thermal loading are investigated. The problem with two edges perpendicular to the fiber direction of the plate, being itself constrained from normal displacement, is first solved analytically. It is then analyzed by the energy method together with the Rayleigh–Ritz approximation, and the computed results are verified by the analytical solution showing very good agreement. Another problem, with two edges parallel to the fiber direction, the plate again being constrained from normal displacement, which is more complex and cannot be solved analytically, is tackled by the afore-mentioned numerical procedure. To investigate the effect of the variation of fiber spacing on the distributions of the displacement-component fields and the equivalent stress field, two types of variation in fiber spacing are assumed in solving the second problem.

Keywords Composite · Rayleigh–Ritz method · Thermal stress · Variable fiber spacing

1 Introduction

Traditionally, flat composite plates are made of laminas, the fibers within each lamina being parallel and uniformly spaced [1]. However, significant increases in structural efficiency may possibly be obtained by varying the fiber spacing. This means packing them more closely together in regions where the higher stiffness is needed, but less densely in other regions.

Although the effect of varying the fiber spacing in flat composite plates is significant, only few relevant efforts have been made up to now. Among them, Fukuka [2] investigated the distribution of stress-concentration factors in a unidirectional composite sheet in which the fiber is randomly spaced. Ochiai and Osamura [3,4] studied the tensile strength and stress distribution in metal-matrix composites with non-uniform fiber spacing. Leissa and Martin [5] applied the Ritz method to solve plane elasticity problems for composite sheets with variable fiber spacing. Leissa and Martin [6] further used the Ritz method to investigate the vibration and buckling of rectangular composite plates with variable fiber spacing, and pointed out that the redistribution of fibers can increase the buckling load by

C.-L. Hwan (✉)
Department of Mechanical and Computer-Aided Engineering, Feng-Chia University,
100 Wenhwa road, Seatween, Taichung, Taiwan
e-mail: clhwan@fcu.edu.tw

as much as 38%, and the fundamental frequency by as much as 21%. Almost at the same time, Leissa and Martin [7] got exact solutions for four types of composite sheet problems with arbitrary fiber spacing.

Aside from that, Pandy [8] studied the effect of varying fiber spacing on the buckling of composite laminates by using the Rayleigh–Ritz method. Shiau and Chue [9] discovered that the free-edge inter-laminar stresses in a symmetric laminate under uniform axial extension can be significantly reduced by varying the fiber volume fraction near the free edge. Shiau and Lee [10] then developed a higher-order triangular plane-stress element to investigate the effect of variable fiber spacing on the stress concentration around a hole in a composite laminated plate subjected to in-plane boundary loadings, and concluded that reducing the fiber volume ratio near the hole edges can significantly reduce the stress concentration in that region.

In addition, Kuo [11] investigated the effect of fiber-volume-fraction variation on buckling strengths and free-vibration frequencies of symmetric composite laminates. Tanaka and his co-workers [12] investigated the influence of the uniformity of geometric fiber arrangement on the fracture behavior of unidirectional fiber-reinforced composites, both experimentally and analytically, and indicated that non-uniform fiber arrangement accelerates the crack growth towards the matrix-rich part.

The studies mentioned above are all assumed isothermal, and no publications concerning thermal effect on the composite plates with variable fiber spacing has been found so far. Because the temperature factor might be crucial in the manufacture of composite plates, especially for composite plates with variable fiber spacing, it ought to initiate a study in this regard.

In the present study, a simple thermal-stress problem of a square composite plate with variable fiber spacing is first solved analytically. The closed-form solution is then used to validate the numerical solution obtained by the Rayleigh–Ritz method. It aims to investigate the effect of non-uniform fiber distribution on the thermal elastic behavior of constrained square composite plates.

2 Elastic properties for parallel-fiber materials with variable fiber spacing

As shown in Fig. 1, the length and width of a composite sheet with non-uniform fiber spacing are denoted by a, and b, respectively. The fibers are aligned parallel to one edge and a xy-coordinate system is chosen with the y-coordinate in the direction of the fibers. The material of such an arrangement can be categorized as orthotropic. When the temperature effect is considered, the stress–strain relationship for an orthotropic sheet under plane-stress condition [1,7] can be written as:

$$\begin{Bmatrix} \sigma_x \\ \sigma_y \\ \tau_{xy} \end{Bmatrix} = \begin{bmatrix} C_{11} & C_{12} & 0 \\ C_{12} & C_{22} & 0 \\ 0 & 0 & C_{66} \end{bmatrix} \left(\begin{Bmatrix} \varepsilon_x \\ \varepsilon_y \\ \gamma_{xy} \end{Bmatrix} - \begin{Bmatrix} \alpha_x \\ \alpha_y \\ 0 \end{Bmatrix} \Delta T \right), \tag{1}$$

where

$$C_{11} = \frac{E_x}{1 - \nu_{yx}\nu_{xy}}, \quad C_{12} = \nu_{yx} C_{11}, \quad C_{22} = \frac{E_y}{1 - \nu_{yx}\nu_{xy}}, \quad C_{66} = G_{xy}. \tag{2,3,4,5}$$

$$\alpha_y = \frac{\alpha_f E_f V_f + \alpha_m E_m V_m}{E_f V_f + E_m V_m}, \quad \alpha_x = V_f(1+\nu_f)\alpha_f + V_m(1+\nu_m)\alpha_m - (\nu_f V_f + \nu_m V_m)\alpha_y. \tag{6,7}$$

In terms of modulus ratios:

$$R_1 = \frac{E_f}{E_m}, \quad R_2 = \frac{\nu_f}{\nu_m}, \quad R_3 = \frac{G_f}{G_m} = \frac{R_1}{R_2}\left(\frac{R_2 + \nu_f}{1 + \nu_f}\right), \quad R_4 = \frac{\alpha_f}{\alpha_m},$$

we can show that

$$E_x = \frac{E_f}{V_f + R_1(1 - V_f)}, \quad E_y = E_f\left(V_f + \frac{1 - V_f}{R_1}\right), \quad \nu_{yx} = \nu_f\left(V_f + \frac{1 - V_f}{R_2}\right), \quad \nu_{xy} = \frac{E_x}{E_y}\nu_{yx}, \tag{8,9,10,11}$$

$$G_{xy} = \frac{E_f}{2(1+\nu_f)[R_3(1-V_f)+V_f]}, \tag{12}$$

$$\alpha_y = \frac{1+(R_1R_4-1)V_f}{1+(R_1-1)V_f}\left(\frac{\alpha_f}{R_4}\right), \quad \alpha_x = \left\{1+V_f(-1+R_4)\left\{1+\frac{(R_1-R_2)(-1+V_f)\nu_f}{R_2[1+(-1+R_1)V_f]}\right\}\right\}\frac{\alpha_f}{R_4}, \tag{13,14}$$

where E_f, ν_f, G_f, α_f and V_f are the longitudinal elastic modulus, Poisson ratio, shear modulus, thermal-expansion coefficient and volume fraction of the fiber, respectively. Correspondingly, E_m, ν_m, G_m, α_m and V_m denote the elastic modulus, Poisson ratio, shear modulus, thermal-expansion coefficient and volume fraction of the matrix material, respectively. Besides, ΔT is the temperature variation, and both V_f and V_m are functions of the x-coordinate.

3 Thermal-elastic formulation of a rectangular composite sheet with variable fiber spacing

3.1 Governing equations

When a composite sheet with non-uniform fiber spacing under a uniform thermal loading, ΔT, is considered, the following governing equations with specified boundary conditions must be satisfied for finding a solution.

Equilibrium equations:

$$\frac{\partial\sigma_x}{\partial x}+\frac{\tau_{xy}}{\partial y}=0, \quad \frac{\partial\sigma_y}{\partial y}+\frac{\tau_{xy}}{\partial x}=0. \tag{15,16}$$

Stress–strain relationships:

$$\sigma_x = C_{11}(\varepsilon_x-\alpha_x\Delta T)+C_{12}(\varepsilon_y-\alpha_y\Delta T), \quad \sigma_y = C_{12}(\varepsilon_x-\alpha_x\Delta T)+C_{22}(\varepsilon_y-\alpha_y\Delta T). \tag{17,18}$$

$$\tau_{xy} = C_{66}\gamma_{xy}, \tag{19}$$

Strain-displacement equations:

$$\varepsilon_x = \frac{\partial u}{\partial x}, \quad \varepsilon_y = \frac{\partial v}{\partial y}, \quad \gamma_{xy} = \frac{\partial u}{\partial y}+\frac{\partial v}{\partial x}. \tag{20,21,22}$$

In addition, the compatibility equation must be satisfied to ensure a continuous configuration of the deformed body:

$$\frac{\partial^2\varepsilon_x}{\partial y^2}+\frac{\partial^2\varepsilon_y}{\partial x^2}=\frac{\partial^2\gamma_{xy}}{\partial x\partial y}. \tag{23}$$

If we first substitute the strain-displacement equations in the stress–strain relationships and then substitute the stress–strain relationships in the equilibrium equations, the following partial differential equations can be obtained:

$$\frac{\partial}{\partial x}\left[C_{11}\left(\frac{\partial u}{\partial x}-\alpha_x\Delta T\right)+C_{12}\left(\frac{\partial v}{\partial y}-\alpha_y\Delta T\right)\right]+\frac{\partial}{\partial y}\left[C_{66}\left(\frac{\partial u}{\partial y}+\frac{\partial v}{\partial x}\right)\right]=0, \tag{24}$$

$$\frac{\partial}{\partial y}\left[C_{12}\left(\frac{\partial u}{\partial x}-\alpha_x\Delta T\right)+C_{22}\left(\frac{\partial v}{\partial y}-\alpha_y\Delta T\right)\right]+\frac{\partial}{\partial x}\left[C_{66}\left(\frac{\partial u}{\partial y}+\frac{\partial v}{\partial x}\right)\right]=0. \tag{25}$$

In general, the above partial differential equations can only be solved to yield a closed form solution for some simple problems. For more complex problems, the energy method, together with a numerical analysis, has to be employed to provide an approximate solution.

3.2 Energy method

As shown in Fig. 1, for a rectangular composite sheet ($a \times b$)under external applied loads and a uniform thermal loading, the total potential energy per unit thickness of the loaded plate, V, is

$$V = V_S - V_L, \tag{26}$$

where the strain energy due to stretching, V_S, and the work done by external applied loads, V_L, can be expressed as

$$V_S = \frac{1}{2}\int_{-a/2}^{a/2}\int_{-b/2}^{b/2}\left[\sigma_x(\varepsilon_x - \alpha_x \Delta T) + \sigma_y(\varepsilon_y - \alpha_y \Delta T) + \tau_{xy}\gamma_{xy}\right]\mathrm{d}x\mathrm{d}y, \tag{27}$$

$$\begin{aligned} V_L = &\int_{-a/2}^{a/2}\left[\sigma_{y0}v + \tau_{xy0}u\right]_{y=b/2}\mathrm{d}x + \int_{-b/2}^{b/2}\left[\sigma_{x0}u + \tau_{xy0}v\right]_{x=a/2}\mathrm{d}y + \int_{-a/2}^{a/2}\left[\sigma_{y0}v + \tau_{xy0}u\right]_{y=-b/2}\mathrm{d}x \\ &+ \int_{-b/2}^{b/2}\left[\sigma_{x0}u + \tau_{xy0}v\right]_{x=-a/2}\mathrm{d}y, \end{aligned} \tag{28}$$

with σ_{x0}, σ_{y0} and τ_{xy0} being components of the force applied on the boundary. Besides, both u and v are components of the displacement vector along the boundary in the x- and y-directions, respectively.

Substituting (17)–(22) in (27) and using the coordinate transformations, $\xi = 2x/a$ and $\eta = 2y/b$ in (27)–(28), we obtain the total potential energy per unit thickness of the loaded square plate (setting $a = b$) as follows:

$$\begin{aligned} V = &\frac{1}{2}\int_{-1}^{1}\int_{-1}^{1}\left[C_{11}\left(\frac{\partial u}{\partial \xi}\right)^2 + 2C_{12}\frac{\partial u}{\partial \xi}\frac{\partial v}{\partial \eta} + C_{22}\left(\frac{\partial v}{\partial \eta}\right)^2 + C_{66}\left(\frac{\partial v}{\partial \xi} + \frac{\partial u}{\partial \eta}\right)^2\right]\mathrm{d}\xi\,\mathrm{d}\eta \\ &- \frac{a\Delta T}{2}\int_{-1}^{1}\int_{-1}^{1}\left[C_{11}\frac{\partial u}{\partial \xi}\alpha_x + C_{12}\left(\frac{\partial v}{\partial \eta}\alpha_x + \frac{\partial u}{\partial \xi}\alpha_y\right) + C_{22}\frac{\partial v}{\partial \eta}\alpha_y\right]\mathrm{d}\xi\,\mathrm{d}\eta + \frac{a^2\Delta T^2}{8}\int_{-1}^{1}\int_{-1}^{1}\left(C_{11}\alpha_x^2\right. \\ &\left. + 2C_{12}\alpha_x\alpha_y + C_{22}\alpha_y^2\right)\mathrm{d}\xi\,\mathrm{d}\eta + \frac{a}{2}\int_{-1}^{1}\left[\sigma_{y0}v + \tau_{xy0}u\right]_{\eta=1}\mathrm{d}\xi + \frac{a}{2}\int_{-1}^{1}\left[\sigma_{y0}v + \tau_{xy0}u\right]_{\eta=-1}\mathrm{d}\xi \\ &+ \frac{a}{2}\int_{-1}^{1}\left[\sigma_{x0}u + \tau_{xy0}v\right]_{\xi=1}\mathrm{d}\eta + \frac{a}{2}\int_{-1}^{1}\left[\sigma_{x0}u + \tau_{xy0}v\right]_{\xi=-1}\mathrm{d}\eta. \end{aligned} \tag{29}$$

The application of the principle of minimum potential energy, together with the Rayleigh–Ritz method, will then provide an approximate solution of the problem to be solved.

4 A simple plane thermal-stress problem of a square plate with variable fiber spacing

As depicted in Fig. 2, a square composite sheet ($a \times a$) with variable fiber spacing is under a uniform thermal loading. The stress-free boundary condition is applied to two opposite edges in the x-direction. The other two edges in the y-direction are constrained from normal displacement, but are free to slide tangentially.

To satisfy the equilibrium equations (15)–(16) and the specified boundary conditions, the following mixed solutions can be assumed to be valid for all x and y:

$$\sigma_x = \tau_{xy} = v = 0; \quad \sigma_y = \sigma_y(x). \tag{30}$$

By using Eq. (21), one normal strain is found from the equation, $v = 0$, to be

$$\varepsilon_y = 0 \tag{31}$$

Then Eqs. (17)–(18), together with Eqs. (30)–(31), give the following two relations:

$$\varepsilon_x = \frac{C_{12}}{C_{11}}\alpha_y \Delta T + \alpha_x \Delta T, \quad \sigma_y = \left(\frac{C_{12}^2}{C_{11}} - C_{22}\right)\alpha_y \Delta T. \tag{32,33}$$

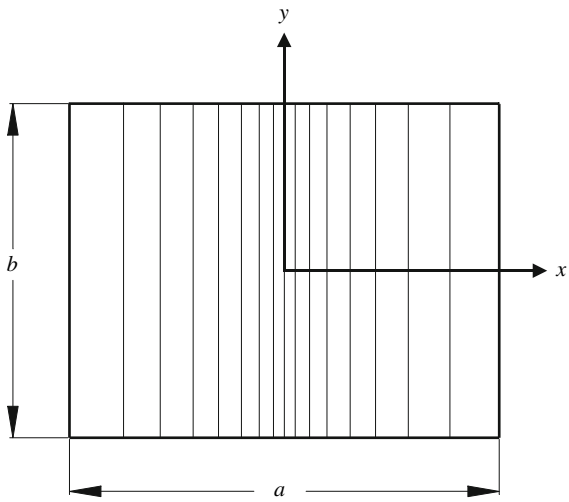

Fig. 1 Schematic diagram of a composite sheet with non-uniform fiber spacing

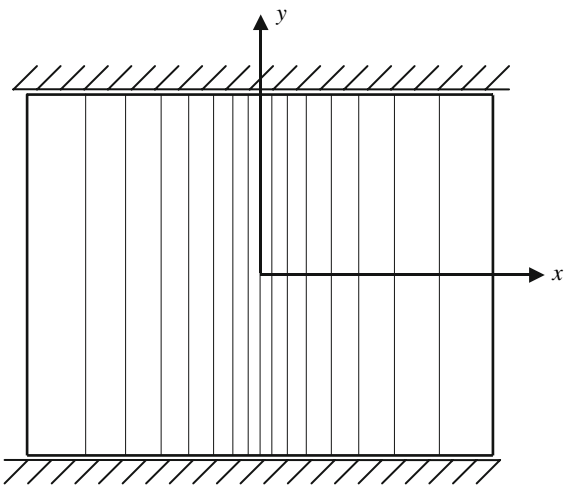

Fig. 2 Boundary conditions for the thermal-stress problem of case I

Employing Eqs. (19) and (30), one gets

$$\tau_{xy} = C_{66}\gamma_{xy} = G_{xy}\gamma_{xy} = 0. \tag{34}$$

Since $C_{66} = G_{xy}$ is nowhere zero, Eq. (34) requires $\gamma_{xy} = 0$ everywhere. Then, according to a procedure similar to that described in [7], we can immediately show that

$$u = \int \varepsilon_x(x)\mathrm{d}x = \int \left(\frac{C_{12}}{C_{11}}\alpha_y + \alpha_x\right)\Delta T\,\mathrm{d}x. \tag{35}$$

Upon substituting the derived stress, strain and displacement fields in the related equations, we can prove that not only the equilibrium equations but also the compatibility equation are exactly satisfied.

Now, the last question remaining is whether the expression for u in (35) can be integrated in closed form. To this end, assuming $V_f = 1 - \xi^2$, $R_1 = 10$, $R_2 = 1$, $\nu_f = 0.25$ and $R_4 = 0.08$ [7,13], we can derive the following equations:

$$C_{11} = \frac{8(-10+9\xi^2)}{3(-25-216\xi^2+216\xi^4)}E_f, \quad C_{12} = \frac{2(-10+9\xi^2)}{3(-25-216\xi^2+216\xi^4)}E_f, \tag{36,37}$$

$$C_{22} = -\frac{4(-10+9\xi^2)^2(1+9\xi^2)}{15(-25-216\xi^2+216\xi^4)}E_f, \quad C_{66} = \frac{2}{5(1+9\xi^2)}E_f, \tag{38,39}$$

$$\alpha_y = \left(\frac{-10-2.5\xi^2}{-10+9\xi^2}\right)\alpha_f, \quad \alpha_x = \left(\frac{-10-131.875\xi^2+129.375\xi^4}{-10+9\xi^2}\right)\alpha_f. \tag{40,41}$$

Substituting (36)–(37) and (40)–(41) in (35), and then integrating, using the symbolic software Mathematica, we end up with a closed-form expression for u:

$$u = a\alpha_f\Delta T\left(0.625\xi + 2.395835\xi^3\right). \tag{42}$$

Again substituting (36)–(38) and (40) in (33), we have

$$\sigma_y = -(1+0.25\xi^2)E_f\alpha_f\Delta T. \tag{43}$$

Substituting (42) in (29), and then integrating by Mathematica, the corresponding total potential energy per unit thickness of the loaded plate can be found as

$$V = 1.237a^2E_f\alpha_f^2\Delta T^2. \tag{44}$$

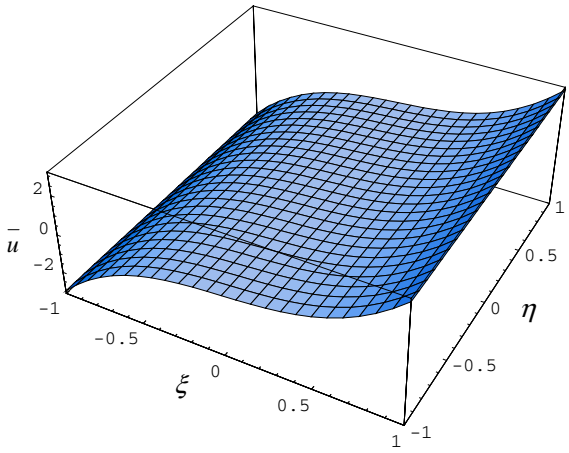

Fig. 3 Distribution of $\overline{u}$ in the composite sheet for $V_f = 1 - \xi^2$

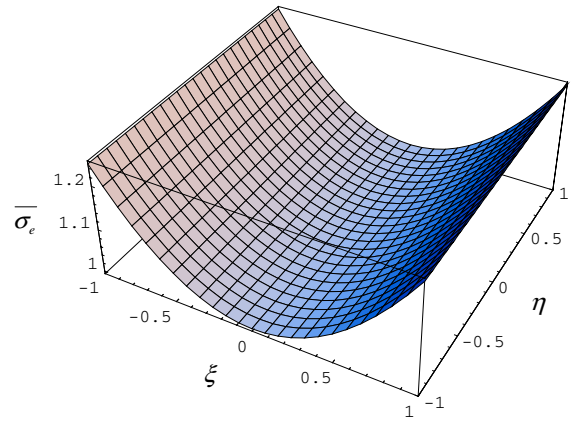

Fig. 4 Distribution of $\overline{\sigma_e}$ in the composite sheet for $V_f = 1 - \xi^2$

Distributions of the normalized displacement component in the x-direction, $\overline{u} = u/a\alpha_f \Delta T$, and the normalized equivalent stress, $\overline{\sigma_e} = \sigma_e / E_f \alpha_f \Delta T$, in the square plate for $V_f = 1 - \xi^2$, are shown in Figs. 3 and 4, where $\sigma_e = \left(\sigma_x^2 + \sigma_y^2 - \sigma_x \sigma_y + 3\tau_{xy}^2\right)^{1/2}$ is the equivalent stress. As depicted in Figs. 3 and 4, both $\overline{u}$ and $\overline{\sigma_e}$ are only functions of ξ and vary with ξ nonlinearly. As for the material distribution, it is fiber-dominated near the center of the square plate, and becomes matrix-dominated near the free edges of the composite plate. Since the thermal-expansion coefficient of matrix is relatively larger than that of fiber, as a result, the absolute value of $\overline{u}$ is getting larger towards the free edges.

5 Numerical analysis and discussion

In this section, two thermal-stress problems of a square plate with variable fiber spacing are solved by the energy method together with the Rayleigh–Ritz method. The computational result of the first problem will be verified by the closed-form solution found above.

5.1 Case I: Plane thermal-stress problem of a square composite sheet with two edges perpendicular to the fiber direction constrained from normal displacement

As shown in Fig. 2, the same problem, stated and solved analytically in the last section, is tackled here again numerically. To apply the Rayleigh–Ritz method for solving the problem [5], the following kinematically admissible displacement fields corresponding to the specified boundary conditions are assumed to be

$$u = \sum_{i=1} \sum_{j=1} A_{ij} \xi^i \eta^j, \quad v = \sum_{k=1} \sum_{l=1} B_{kl} \xi^k \eta^l \left(1 - \eta^2\right). \tag{45,46}$$

Upon substituting $C_{11}, C_{12}, C_{22}, C_{66}, \alpha_x, \alpha_y, u$ and v, namely Eqs. (36)–(41) and Eqs. (45)–(46), in (29), we may form an expression for the total potential energy per unit thickness of the loaded plate by a numerical integration with 16 integration points [14]. Such an expression is a function of the unknown coefficients A_{ij} and B_{kl}.

To consider the symmetry of the problem for finding an approximate solution more efficiently [5], the principle of minimum potential energy is then applied which requires

$$\frac{\partial V}{\partial A_{ij}} = 0 \quad (i = 1, 3, \ldots, (2I - 1);\ j = 0, 2, \ldots, (2J - 2)) \tag{47}$$

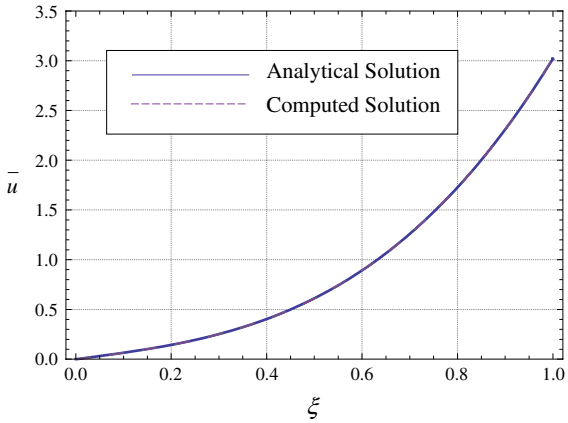

Fig. 5 A comparison of the computed $\overline{u}$ and the analytical $\overline{u}$ in the composite sheet

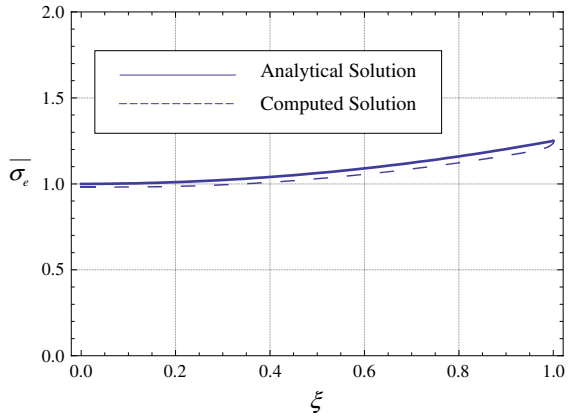

Fig. 6 A comparison of the computed $\overline{\sigma_e}$ and the analytical $\overline{\sigma_e}$ in the composite sheet

and

$$\frac{\partial V}{\partial B_{kl}} = 0 \quad (k = 0, 2, \ldots, (2K-2); l = 1, 3, \ldots, (2L-1)) . \tag{48}$$

Equations (47)–(48) generate $(I \times J) + (K \times L)$ simultaneous algebraic equations, which can be solved to provide the unknown coefficients A_{ij} and B_{kl} [15]. Now the displacement-component fields and the total potential energy per unit thickness can be calculated upon substituting A_{ij} and B_{kl} in (45)–(46) and (29). All the calculations mentioned above were done by Mathematica.

For the present study, $I = J = K = L = 7$ are used to generate 98 simultaneous algebraic equations. They are then solved to provide an approximate solution. The distributions of the computed normalized displacement component, $\overline{u}$, and the computed generalized equivalent stress, $\overline{\sigma_e}$, are very similar to those depicted in Figs. 3 and 4 from the analytical solution. For a more distinct comparison, both the analytical and computed results of $\overline{u}$ and $\overline{\sigma_e}$ at $\eta = 0$ are plotted as functions of ξ in Figs. 5 and 6 for ξ from 0 to 1 due to symmetry. It is found from Fig. 5 that the curve of the computed $\overline{u}$ coincides exactly with that of the analytical solution because $\overline{u}$ is the primary variable which must satisfy the boundary conditions to be kinematically admissible. However, there exists some insignificant discrepancy between curves of both the computed $\overline{\sigma_e}$ and the analytical $\overline{\sigma_e}$, as illustrated by Fig. 6, because the components of the stress tensor are secondary or derived variables in the computation. Moreover, the computed total potential energy per unit thickness, $V = 1.237 a^2 E_f \alpha_f^2 \Delta T^2$, is closely in congruence with the value obtained by the analytical procedure.

5.2 Case II: The plane thermal-stress problem of a square composite sheet with two edges parallel to the fiber direction constrained from normal displacement

As depicted in Fig. 7, a square composite sheet $(a \times a)$ with variable fiber spacing is under a uniform thermal loading. The stress-free boundary condition is applied to two opposite edges in the y-direction. The other two edges in the x-direction are constrained from normal displacement, but are free to slide tangentially. This problem can not be solved analytically and has been worked out numerically.

To solve the problem [5] by the Rayleigh–Ritz method, the kinematically admissible displacement fields corresponding to the specified boundary conditions were assumed to be

$$u = \sum_{i=1} \sum_{j=1} A_{ij} \xi^i \eta^j \left(1 - \xi^2\right), \quad v = \sum_{k=1} \sum_{l=1} B_{kl} \xi^k \eta^l . \tag{49,50}$$

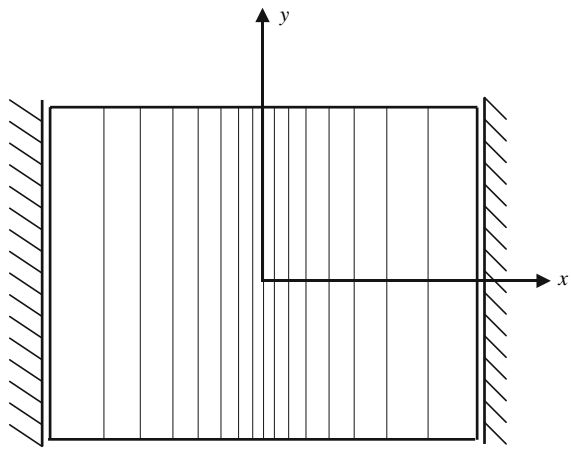

Fig. 7 Boundary conditions for the thermal-stress problem of case II

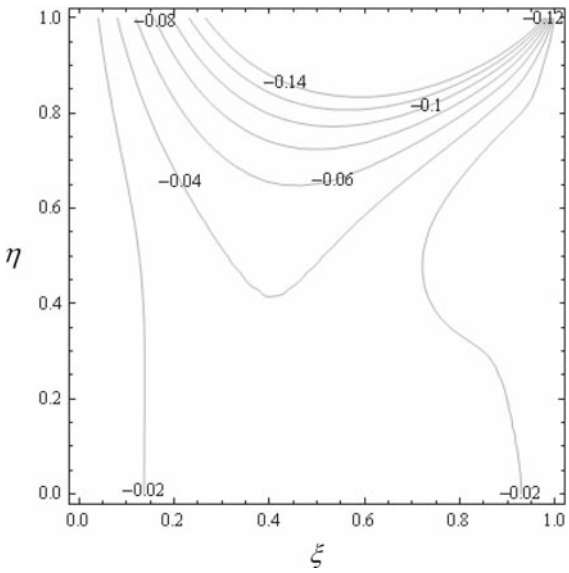

Fig. 8 The contour of $\overline{u}$ for the problem of Case II, $V_f = 1-\xi^2$

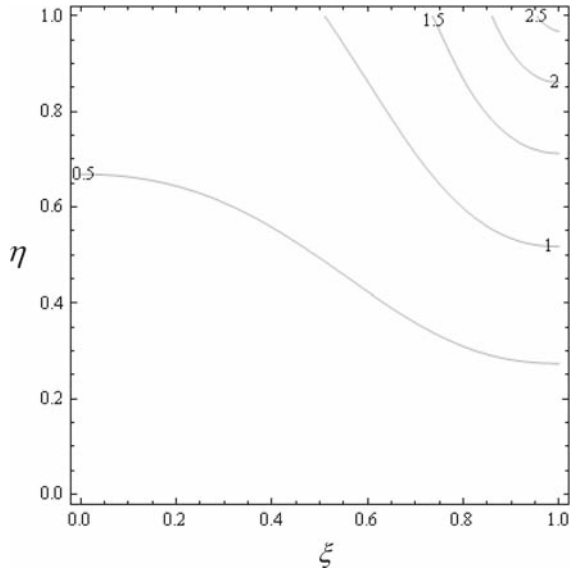

Fig. 9 The contour of $\overline{v}$ for the problem of Case II, $V_f = 1-\xi^2$

Following the same procedure as mentioned in Sect. 5.1, the normalized displacement-component fields, $\overline{u}$ and $\overline{v} = v/a\alpha_f\Delta T$, and the normalized equivalent stress field, $\overline{\sigma_e}$, for $V_f = 1-\xi^2$ were then calculated. Due to the symmetry of the problem with respect to both the x-and y-axes, only the results in the first quadrant of the computational domain are plotted in Figs. 8–10.

As shown in Figs. 8 and 9, the distributions of both $\overline{u}$ and $\overline{v}$ are significantly non-uniform. Due to the constraints on the edges parallel to the fiber direction, the order of magnitude of $\overline{u}$ is obviously less than that of $\overline{v}$. There exists a region near the free edge ($\eta = 1$) where the gradient of $\overline{u}$ is more obvious as described by Fig. 8. As the distribution of fiber near the constrained edge ($\xi = 1$) is the least, the material near the constrained edge is mainly composed of matrix. Since the thermal-expansion coefficient of matrix is much larger than that of fiber, as a result, the largest amount of deformation under a uniform thermal loading occurs near the constrained edge, and thus induces the largest displacement approximately at the corner ($\xi = 1, \eta = 1$) as shown in Fig. 9.

In addition, as is evident from Fig. 10, the distribution of $\overline{\sigma_e}$ is also very non-uniform. It is found that the least value of $\overline{\sigma_e}$ occurs almost at the corner ($\xi = 1, \eta = 1$), and the largest value of $\overline{\sigma_e}$ occurs approximately at the midpoint of the free edge ($\xi = 0, \eta = 1$).

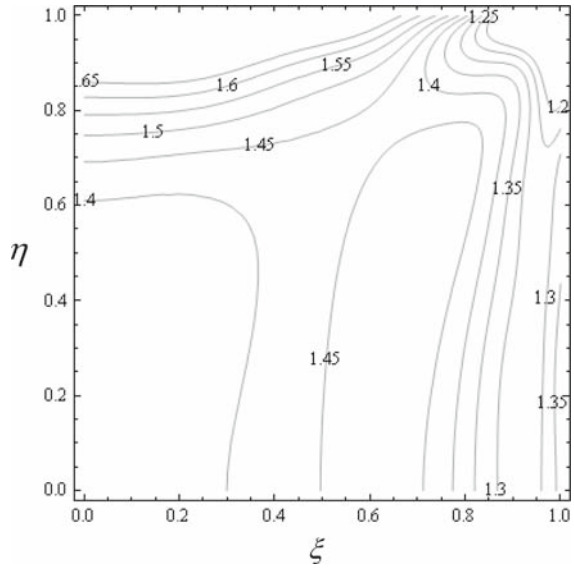

Fig. 10 The contour of $\overline{\sigma_e}$ for the problem of Case II, $V_f = 1 - \xi^2$

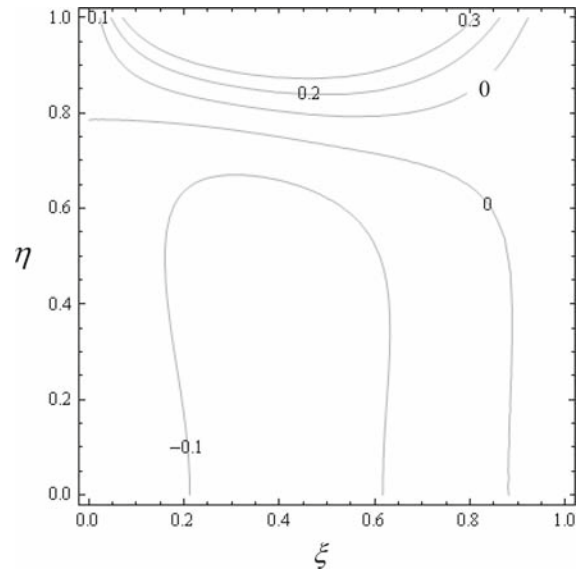

Fig. 11 The contour of $\overline{u}$ for the problem of Case II, $V_f = \xi^2$

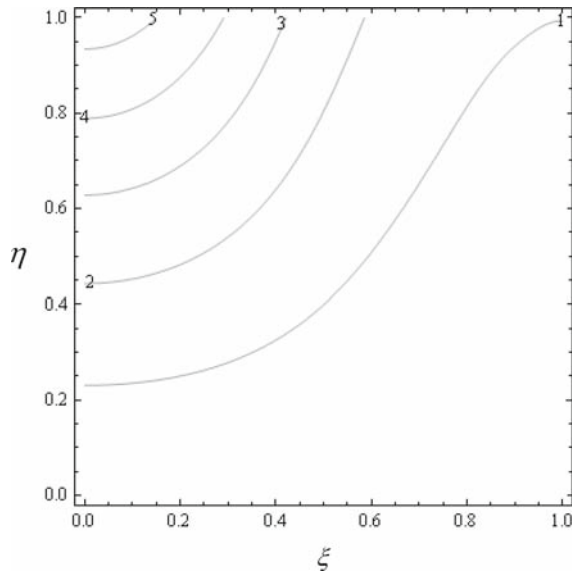

Fig. 12 The contour of $\overline{v}$ for the problem of Case II, $V_f = \xi^2$

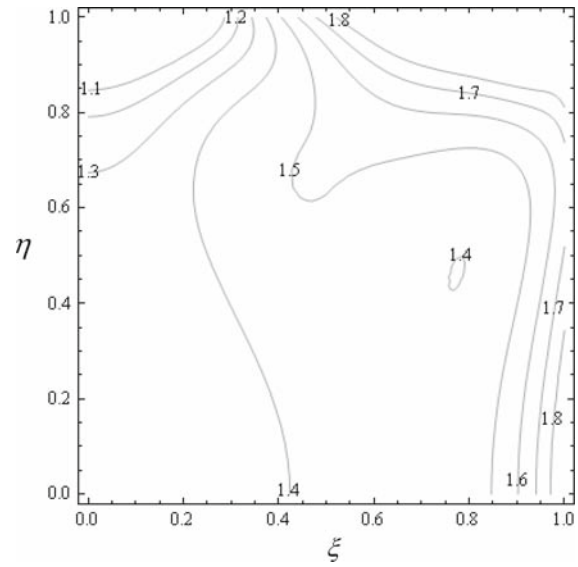

Fig. 13 The contour of $\overline{\sigma_e}$ for the problem of Case II, $V_f = \xi^2$

To investigate the effect of fiber spacing on the deformation and thermal stress of the square composite sheet, a different variation of fiber-volume fraction is assumed to be $V_f = \xi^2$. With this fiber distribution, the material at the plate center is all matrix, whereas at the edges, $\xi = \pm 1$, it is all fiber. The computed displacement-component fields, $\overline{u}$ and $\overline{v}$, and the equivalent stress field, $\overline{\sigma_e}$ for $V_f = \xi^2$ are plotted in Figs. 11–13.

As depicted in Figs. 11 and 12, the distributions of both $\overline{u}$ and $\overline{v}$ are strongly nonlinear. Because the edges parallel to fiber direction are constrained from normal displacement, as a result, the order of the magnitude of $\overline{u}$ is obviously less than that of $\overline{v}$. There also exists a region near the free edge where the gradient of $\overline{u}$ is more obvious as described by Fig. 11. As the distribution of fiber at $\xi = 0$ is the least, the material near the η-axis is mainly composed of matrix. As a consequence, the largest amount of deformation under a uniform thermal

loading occurs near the η-axis, and thus induces the largest displacement approximately at the midpoint of the free edge ($\xi = 0, \eta = 1$) as illustrated in Fig. 12.

Besides, as shown in Fig. 13, the distribution of $\overline{\sigma_e}$ also varies nonlinearly. Contrary to that in Fig. 10, it is found that the largest value of $\overline{\sigma_e}$ occurs approximately near the corner ($\xi = 1, \eta = 1$) and the lowest value of $\overline{\sigma_e}$ occurs almost at the midpoint of the free edge ($\xi = 0, \eta = 1$).

6 Conclusions

We have investigated plane thermal-stress problems of a square composite plate with variable fiber spacing both analytically and computationally. When two edges perpendicular to the fiber direction of the plate are constrained from normal displacement, it is found that the plate will only deform in the transverse direction under a uniform thermal loading. Both $\overline{u}$ and $\overline{\sigma_e}$ increase with the increase of ξ, and become the largest near free edges. However, when the other two edges, parallel to the fiber direction, are constrained from normal displacement, the deformation of the plate under a uniform thermal loading becomes much more complicated. In this case, numerical results show that the plate will deform not only in the fiber direction but also in the transverse direction. The distributions of $\overline{u}$ $\overline{v}$ and $\overline{\sigma_e}$ are not uniform and very complex.

In the region with the smaller fiber-volume fraction, the deformation of the plate is more significant because it is dominated by the larger thermal-expansion coefficient of matrix. On the other hand, the equivalent stress is the larger in the area with the larger fiber-volume fraction because it is affected by the stronger stiffness of fiber.

References

1. Gibson RF (1994) Principles of composite material mechanics. McGraw-Hill, Singapore
2. Fukuda H (1985) Stress concentration factors in unidirectional composites with random fiber spacing. Compos Sci Technol 22:153–163
3. Osamura K, Ochiai S (1989) Tensile strength of fiber-reinforced metal matrix composites with non-uniform fiber spacing. J Mater Sci Technol 24:3536–3540
4. Osamura K, Ochiai S (1989) Stress disturbance due to broken fibers in metal matrix composites with non-uniform fibre spacing. J Mater Sci Technol 24:3865–3872
5. Martin AF, Leissa AW (1989) Application of the Ritz method to plane elasticity problems for composite sheets with variable fiber spacing. Int J Numer Meth Eng 28:1813–1825
6. Leissa AW, Martin AF (1990) Vibration and buckling of rectangular composite plates with variable fiber spacing. Compos Struct 14:339–357
7. Leissa AW, Martin AF (1990) Some exact plane elasticity solutions for nonhomogeneous, orthotropic sheets. J Elasticity 23: 97–112
8. Pandy MD (1991) Structure-material interaction in stability of fibrous composite elements. PhD dissertation, Waterloo University
9. Shiau LC, Chue Y H (1991) Free-edge stress reduction through fiber volume fraction variation. Compos Struct 19:145–165
10. Shiau LC, Lee GC (1993) Stress concentration around holes in composite laminates with variable fiber spacing. Compos Struct 24:107–115
11. Kuo CF (1995) Buckling and vibrational behaviors of composite laminates with variable fiber spacing. MS Thesis, National Cheng-Kung University, Taiwan
12. Tanaka M, Hojo M, Hobbiebrunken T, Ochiai S, Hirosawa Y, Fujita K, Sawada Y (2005) Influence of non-uniform fiber arrangement on tensile fracture behavior of unidirectional fiber/epoxy model composites. Compos Interfaces 12:365–378
13. Hull D, Clyne TW (1996) An introduction to composite materials. Cambridge University Press
14. Abramowitz M, Stegun IA (1972) Handbook of mathematical functions with formulas, graphs, and mathematical tables. U. S. Govt. Print Office
15. Carnahan B, Luther HA, Wilkes JO (1969) Applied numerical methods. John-Wiley and Sons, Inc.